

Spin-textures of the Bose-Einstein condensates with three kinds of spin-1 atoms

Y. Z. He¹, Y. M. Liu², and C. G. Bao^{1,*}

¹School of Physics, Sun Yat-Sen University, Guangzhou, 510275, P. R. China

²Department of physics, Shaoguan University, shaoguan, 510205, P. R. China

*Corresponding author: C.G. Bao, stsbcg@mail.sysu.edu.cn

ABSTRACT

We have performed a quantum mechanic calculation (including solving the coupled Gross-Pitaevskii equations to obtain the spatial wave functions, and diagonalizing the spin-dependent Hamiltonian in the spin-space to obtain the total spin state) together with an analytical analysis based on a classical model. Then, according to the relative orientations of the spins S_A , S_B and S_C of the three species, the spin-textures of the ground state can be classified into two types. In Type-I the three spins are either parallel or anti-parallel to each others, while in Type-II they point to different directions but remain to be coplanar. Moreover, according to the magnitudes of S_A , S_B and S_C the spin-textures can be further classified into four kinds, namely, $p+p+p$ (all atoms of each species are in singlet-pairs), one species in f (fully polarized) and two species in q (a mixture of polarized atoms and singlet-pairs), two in f and one in q , and $f+f+f$. Other combinations are not allowed. The scopes of the parameters that supports a specific spin-texture have been specified. A number of spin-texture-transitions have been found. For Type-I, the critical values at which a transition takes place are given by simple analytical formulae, therefore these values can be predicted.

Introduction

The study of the multi-species Bose-Einstein condensates (BEC) with atoms having nonzero spin is an attractive topic. For these systems, when the temperature is extremely low (say, lower than 10^{-9} K), the spatial degrees of freedom are nearly frozen and the spin degrees of freedom play essential roles. Various spin-textures will emerge, and they are found to be sensitive to the very weak spin-dependent forces. Therefore, these systems might be ideal for realizing exquisite control.

When the BEC contains only one kind of N spin-1 atoms, the polar phase (p -phase) and the ferromagnetic phase (f -phase) have been found in the ground state (g.s.)¹⁻⁶. In the p -phase the spins of atom are two-by-two coupled to zero to form the singlet pairs (s -pair), and the total spin of the condensate $S = 0$. In the f -phase all the spins are fully polarized, i.e., lying along a common direction, and $S = N$. For 2-species BEC it was found in⁷⁻¹⁷ that there are three types of spin-textures, namely, (i) the $p+p$ texture where both species are in p -phase; (ii) the $f//f$ texture where both species are in f -phase, and the two total spins (each for a species) are lying either parallel or antiparallel to each other; and (iii) the $f//q$ texture where one in f -phase and one in quasi-ferromagnetic phase (q -phase, a mixture of aligned spins and s -pairs).

The above message from 2-species BEC attracts the exploration on the spin-textures of multi-species BEC. Note that, for 3-species BEC, the three intra-species and three inter-species spin-dependent interactions can be repulsive or attractive. Thus, the spin-textures are expected to be very rich. However, this interesting topic is scarcely studied before. This paper is a primary study on this topic. The aim is to clarify the variety of the spin-textures and the related critical phenomena, and the effects of the intra- and inter-species interactions. We believe that the knowledge extracted from 3-species BEC would be in general useful for understanding the spin-textures of many-body systems with multi-species.

We proceed in the following way:

- From the experience of 2-species BEC, the spin-textures are seriously affected by the compactness of the spatial wave functions (i.e., $\int \varphi_A^4 d\mathbf{r}$ and $\int \varphi_B^4 d\mathbf{r}$) and the overlap (i.e., $\int \varphi_A^2 \varphi_B^2 d\mathbf{r}$). For 3-species BEC, $\int \varphi_J^4 d\mathbf{r}$ ($J = A, B, C$) and $\int \varphi_J^2 \varphi_{J'}^2 d\mathbf{r}$ are believed to be also important. Therefore, we solve the coupled Gross-Pitaevskii equations (CGP) under the Thomas-Fermi approximation (TFA) to obtain the spatial wave functions. It is well known that the TFA cannot correctly describe the tails of the wave functions. However, when the particle numbers are huge, the gross feature given by the TFA is good. Since only the gross feature is concerned, the TFA is acceptable.
- Let S_J be the total spin of the J -species. When the singlet-pairing force has been neglected, the three $\{S_J\}$ together with the total spin S of the mixture are good quantum numbers is the total spin-states Ξ . Ξ is obtained via a diagonalization

of the Hamiltonian in the spin-space. In order to extract physical features from Ξ , in addition to the good quantum numbers, the averaged angles $\bar{\theta}_{JJ'}$ between S_J and $S_{J'}$ have also been calculated. Thereby various types of spin-textures specified by $\{S_J\}$ and $\{\bar{\theta}_{JJ'}\}$ can be identified. and the transitions among them are found.

- In addition to the above quantum mechanic (QM) calculation, a corresponding classical model has been proposed and solved analytically. The results from the model are checked via a comparison with those from QM calculation. This model helps greatly to understand the complicated 3-species spin-textures

Hamiltonian and the ground state

We consider that the condensate is a mixture of three kinds of spin-1 atoms with particle numbers N_J ($J = A, B$ or C), and they are trapped by isotropic and harmonic potentials $\frac{1}{2}m_J\omega_J^2r^2$. The intra-species interaction is $V_J = \sum_{1 \leq i < j \leq N_J} \delta(\mathbf{r}_i - \mathbf{r}_j)(c_{J0} + c_{J2}\mathbf{F}_i^J \cdot \mathbf{F}_j^J)$, where \mathbf{F}_i^J is the spin operator of the i -th atom of the J -species. The inter-species interaction is $V_{JJ'} = \sum_{1 \leq i \leq N_J} \sum_{1 \leq j \leq N_{J'}} \delta(\mathbf{r}_i - \mathbf{r}_j)(c_{JJ'0} + c_{JJ'2}\mathbf{F}_i^J \cdot \mathbf{F}_j^{J'})$. We introduce two quantities m and ω , and use $\hbar\omega$ and $\lambda \equiv \sqrt{\hbar/(m\omega)}$ as the units for energy and length. Then, the total Hamiltonian is

$$H = \sum_J (\hat{K}_J + V_J) + \sum_{J < J'} V_{JJ'}, \quad (1)$$

where $\hat{K}_J = \sum_{i=1}^{N_J} \hat{h}_J(i)$, $\hat{h}_J(i) = \frac{1}{2}(-\frac{m}{m_J}\nabla_i^2 + \gamma_J r_i^2)$ and $\gamma_J = \frac{m_J\omega_J^2}{m\omega^2}$.

Note that, in the ground state (g.s.), every particles of a kind will condense to a spatial state (say, φ_J) which is most favorable for binding. Let Ξ denotes a normalized total spin-state. Then the g.s. can be in general written as

$$\Psi_0 = \prod_{i=1}^{N_A} \varphi_A(\mathbf{r}_i) \prod_{j=1}^{N_B} \varphi_B(\mathbf{r}_j) \prod_{k=1}^{N_C} \varphi_C(\mathbf{r}_k) \Xi. \quad (2)$$

Let $\vartheta_{S_J M_J}^{N_J}$ denote a normalized and all-symmetric spin-state for the J -species where the spins are coupled to S_J and its Z -component M_J . According to the theory given in¹⁸, $N_J - S_J$ must be even, the multiplicity of $\vartheta_{S_J M_J}^{N_J}$ is one (i.e., $\vartheta_{S_J M_J}^{N_J}$ is unique when S_J and M_J are fixed), and the set $\{\vartheta_{S_J M_J}^{N_J}\}$ is complete for all-symmetric spin-states. Let $(\vartheta_{S_A}^{N_A} \vartheta_{S_B}^{N_B})_{S_{AB} M_{AB}} \equiv (S_A S_B)_{S_{AB} M_{AB}}$ be a combined spin-state of the A and B -species, in which S_A and S_B are coupled to S_{AB} and M_{AB} . Let $((\vartheta_{S_A}^{N_A} \vartheta_{S_B}^{N_B})_{S_{AB}} \vartheta_{S_C}^{N_C})_{S M} \equiv ((S_A S_B)_{S_{AB}} S_C)_{S M}$ be a total spin-state of the mixture, in which S_{AB} and S_C are coupled to S and M . When the Hamiltonian is given as above, it turns out that S_A, S_B, S_C, S and M are good quantum numbers, but S_{AB} is not. Nonetheless, the states $((S_A S_B)_{S_{AB}} S_C)_{S M}$ form a complete set so that Ξ can be expanded by them.

The coupled Gross-Pitaevskii equations and the spatial wave functions

For the Hamiltonian given in Eq.(1), based on a standard variational approach we can obtain the set of CGP equations for φ_A to φ_C as⁷

$$(\hat{h}_A + \alpha_{AA}\varphi_A^2 + \alpha_{AB}\varphi_B^2 + \alpha_{CA}\varphi_C^2 - \varepsilon_A)\varphi_A = 0 \quad (3)$$

$$(\hat{h}_B + \alpha_{AB}\varphi_A^2 + \alpha_{BB}\varphi_B^2 + \alpha_{BC}\varphi_C^2 - \varepsilon_B)\varphi_B = 0 \quad (4)$$

$$(\hat{h}_C + \alpha_{CA}\varphi_A^2 + \alpha_{BC}\varphi_B^2 + \alpha_{CC}\varphi_C^2 - \varepsilon_C)\varphi_C = 0 \quad (5)$$

where φ_A, φ_B and φ_C are required to be normalized.

Since the spin-dependent forces are in general two order weaker than the central forces, as a reasonable approximation, the contribution of the former on the set $\{\alpha_{JJ'}\}$ can be neglected. Then, we have $\alpha_{JJ'} = c_{J0}N_J$ (if $J = J'$) or $\alpha_{JJ'} = c_{JJ'0}N_{J'}$ (if $J \neq J'$).

Since the kinetic energy increases linearly with particle number N , while the interaction energy increases with N^2 , the relative importance of the kinetic terms is very weak when N is very large. In this case, the TFA is a reasonable approximation¹⁹⁻²¹. By neglecting the kinetic terms, in a domain where all the φ_J are nonzero, the CGP can be written in a matrix form as

$$\mathfrak{M} \begin{pmatrix} \varphi_A^2 \\ \varphi_B^2 \\ \varphi_C^2 \end{pmatrix} = \begin{pmatrix} \varepsilon_A - \gamma_A r^2/2 \\ \varepsilon_B - \gamma_B r^2/2 \\ \varepsilon_C - \gamma_C r^2/2 \end{pmatrix}, \quad (6)$$

where \mathfrak{M} is a 3×3 matrix with elements $\alpha_{JJ'}$. Let the determinant of \mathfrak{M} be \mathfrak{D} . From the above matrix equation, we obtain a formal solution of the CGP as

$$\varphi_J^2 = Z_J - Y_J r^2, \quad (J = A, B, C) \quad (7)$$

$$Z_J = \mathfrak{D}_J^Z / \mathfrak{D}. \quad (8)$$

\mathfrak{D}_J^Z is a determinant obtained by changing the J column of \mathfrak{D} from $(\alpha_{AJ}, \alpha_{BJ}, \alpha_{CJ})$ to $(\varepsilon_A, \varepsilon_B, \varepsilon_C)$.

$$Y_J = \mathfrak{D}_J^Y / \mathfrak{D}. \quad (9)$$

\mathfrak{D}_J^Y is also a determinant obtained by changing the J column of \mathfrak{D} to $(\gamma_A/2, \gamma_B/2, \gamma_C/2)$. Once all the parameters are given, the three Y_J are known because they depend only on $\alpha_{JJ'}$ and γ_J . However, the three Z_J have not yet been known because they depend on $(\varepsilon_A, \varepsilon_B, \varepsilon_C)$. When Y_J is positive (negative), φ_J^2 goes down (up) with r . Thus the main feature of this formal solution depends on the signs of the set $\{Y_J\}$.

The set $\{Z_J\}$ and the set $\{\varepsilon_J\}$ are related as

$$\varepsilon_J = \sum_{J'} \alpha_{JJ'} Z_{J'}, \quad (10)$$

$$Z_J = \sum_{J'} \bar{\alpha}_{JJ'} \varepsilon_{J'}. \quad (11)$$

where $\bar{\alpha}_{JJ'} = \mathfrak{d}_{J'J} / \mathfrak{D}$, and $\mathfrak{d}_{J'J}$ is the algebraic cominor of $\alpha_{JJ'}$. This formal solution is named the Form III, which is valid only in a domain where all the three φ_J are nonzero.

When two wave functions are nonzero inside a domain while the third is zero, in a similar way we obtain

$$\begin{cases} \varphi_l^2 = Z_l^{(n)} - Y_l^{(n)} r^2 \\ \varphi_m^2 = Z_m^{(n)} - Y_m^{(n)} r^2 \\ \varphi_n^2 = 0 \end{cases}, \quad (12)$$

where l, m and n are a cyclic permutation of A, B and C .

$$\begin{cases} Z_l^{(n)} = (\alpha_{mm} \varepsilon_l - \alpha_{lm} \varepsilon_m) / \mathfrak{d}_{nn} \\ Y_l^{(n)} = \frac{1}{2} (\alpha_{mm} - \alpha_{lm}) / \mathfrak{d}_{nn} \\ Z_m^{(n)} = (\alpha_{ll} \varepsilon_m - \alpha_{ml} \varepsilon_l) / \mathfrak{d}_{nn} \\ Y_m^{(n)} = \frac{1}{2} (\alpha_{ll} - \alpha_{ml}) / \mathfrak{d}_{nn} \end{cases} \quad (13)$$

Once the parameters are given, the six $Y_{n'}^{(n)}$ ($n' \neq n$) are known, while the six $Z_{n'}^{(n)}$ have not yet. This formal solution with $\varphi_n = 0$ is denoted as Form II $_n$, where the subscript specifies the vanishing wave function.

When one and only one of the wave functions is nonzero in a domain (say, $\varphi_J \neq 0$), it must have the unique form as

$$\varphi_J^2 = \frac{1}{\alpha_{JJ}} (\varepsilon_J - \gamma_J r^2 / 2). \quad (14)$$

Obviously, φ_J in this form must descend with r . This form is denoted as Form I $_J$, where the subscript specifies the survived wave function.

If a wave function (say, φ_J) is nonzero in a domain but becomes zero when $r \geq r_0$, then a downward form-transition (say, from Form III to II $_J$) will occur at r_0 . Whereas if φ_J is zero in a domain but emerges from zero when $r \geq r_0$, then an upward form-transition (say, from Form II $_J$ to III) will occur at r_0 . r_0 appears as the boundary separating the two connected domains, each supports a specific form. In this way the formal solutions serve as the building blocks, and they will link up continuously to form an entire solution of the CGP. They must be continuous at the boundary because the two sets of wave functions by the two sides of the boundary satisfy exactly the same set of nonlinear equations at the boundary.

Recall that there are three unknowns $\varepsilon_A, \varepsilon_B$ and ε_C contained in the formal solutions. Taking the three additional equations of normalization $\int \varphi_J^2 dr = 1$ into account, the three unknowns can be obtained. Then, under the TFA, the CGP is completely solved. The details are shown below.

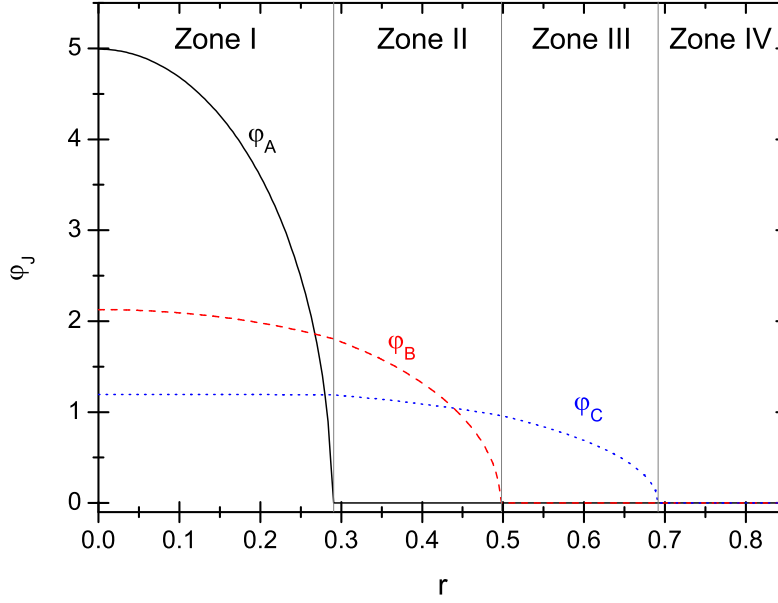


Figure 1. (color online) An example of the spatial wave functions of a miscible state obtained from the TFA solution of the CGP. The parameters are given as $Y_A = 300$, $Y_B = 15$, $Y_C = 0.1$, $Y_B^{(A)} = 20$, $Y_C^{(A)} = 3$, $\alpha_{CC} = 0.01$ and $\gamma_C = 0.08$.

The spatial wave functions

Note that the variety of the spin-textures in multi-species BEC is caused by the inter-species interactions. Obviously, they will play a more essential role when the three kinds of atoms are distributed closer to each other. Therefore, in the following examples, we take the miscible states into account, in which all the three species have nonzero distribution at the center ($r = 0$). An example is given in Fig.1, where the wave functions in zone I to IV are in Form III, Form II₁, Form I₃, and empty, respectively.

For this example, we know that the boundary r_a (at which $\varphi_A = 0$) is equal to $\sqrt{Z_A/Y_A}$ (refer to Eq.(7)), r_b (at which $\varphi_B = 0$) is equal to $\sqrt{Z_B^{(A)}/Y_B^{(A)}}$ (Eq.(12)), r_c (at which $\varphi_C = 0$) is equal to $\sqrt{2\varepsilon_C/\gamma_C}$ (Eq.(14)). They give the outmost boundary of φ_A , φ_B and φ_C , respectively. Taking the normalization into account, we obtain

$$Z_A = \left(\frac{15}{8\pi}\right)^{2/5} Y_A^{3/5}, \quad (15)$$

$$Z_B^{(A)} = \left(\frac{15}{8\pi}\right)^{2/5} (Y_B^{(A)})^{3/5} [1 - (Y_B - Y_B^{(A)})/Y_A]^{2/5}, \quad (16)$$

$$Z_B = Z_B^{(A)} + \left(\frac{15}{8\pi}\right)^{2/5} (Y_B - Y_B^{(A)})/Y_A^{2/5}, \quad (17)$$

$$\varepsilon_C/\alpha_{CC} = \left(\frac{15}{8\pi}\right)^{2/5} \left(\frac{\gamma_C}{2\alpha_{CC}}\right)^{3/5} \left[1 - \frac{Y_C - Y_C^{(A)}}{Y_A} - (Y_C^{(A)} - \frac{\gamma_C}{2\alpha_{CC}}) \frac{1}{Y_B^{(A)}} \left(1 - \frac{Y_B - Y_B^{(A)}}{Y_A}\right)\right]^{2/5}, \quad (18)$$

$$Z_C^{(A)} = \frac{\varepsilon_C}{\alpha_{CC}} + (Y_C^{(A)} - \frac{\gamma_C}{2\alpha_{CC}}) \frac{Z_B^{(A)}}{Y_B^{(A)}}, \quad (19)$$

$$Z_C = Z_C^{(A)} + (Y_C - Y_C^{(A)}) \left(\frac{15}{8\pi Y_A}\right)^{2/5}. \quad (20)$$

Since Z_A , Z_B , and Z_C have been obtained as given above, ε_A and ε_B can be further obtained via Eq.(10). Then, the entire solution of the CGP together with the chemical potentials are completely known.

Nonetheless, the realization of the miscible state is based on a number of assumptions. First, it is assumed that all the wave functions are nonzero at the center, thus $Z_A > 0$, $Z_B > 0$, and $Z_C > 0$ are required. Second, φ_A is assumed to descend with r in zone I and φ_B is assumed to descend with r in zone II, thus $Y_A > 0$ and $Y_B^{(A)} > 0$ are required. Third, $\varphi_B|_{r_a} > 0$ and $\varphi_C|_{r_a} > 0$ are required so that the Form III can link with a Form II_A at r_a . Fourth, $\varphi_C|_{r_b} > 0$ is required so that the Form II_A can link with a Form I_C at r_b . Each of these requirements will impose a constraint on the parameters (say, the requirement $\varphi_B|_{r_a} > 0$ leads

to $Z_B^{(A)} > Y_B^{(A)} r_a^2$, and therefore leads to $Y_A > Y_B$). Thus, the type as shown in Fig.1 can be realized only if the parameters are given inside a specific scope. A comprehensive discussion on the scope of parameters for each spatial type of solution is the base for obtaining the phase-diagrams, but this is beyond the scope of this paper.

The total spin-state

Recall that, in the spin-space, Ξ can be expanded via the basis-states $((S_A S_B)_{S_{AB}} S_C)_{SM}$, where S_A, S_B, S_C, S and M are good quantum numbers, and S_{AB} is ranged from $|S_A - S_B|$ to $S_A + S_B$. Taking the spatial states into account, we define a set of basis-states for the g.s. as

$$\Psi_{\mathfrak{S}, S_{AB}} = \prod_{i=1}^{N_A} \varphi_A(\mathbf{r}_i) \prod_{j=1}^{N_B} \varphi_B(\mathbf{r}_j) \prod_{k=1}^{N_C} \varphi_C(\mathbf{r}_k) ((S_A S_B)_{S_{AB}} S_C)_{SM}. \quad (21)$$

where the subscript \mathfrak{S} denotes a specific set $(S_A S_B S_C S)$. When a magnetic field is not applied, the label M can be neglected. Accordingly, a candidate of the g.s. can be expanded as

$$\Psi_{\mathfrak{S}} = \sum_{S_{AB}} d_{S_{AB}} \Psi_{\mathfrak{S}, S_{AB}}, \quad (22)$$

Let H be divided as $H = H_0 + H_{\text{spin}}$, where all the spin-dependent interactions are included in H_{spin} . Let (J_-, J, J_+) be a cyclic permutation of (A, B, C) . Then $H_{\text{spin}} = \sum_J c_{J2} \sum_{1 \leq i < j \leq N_J} \delta(\mathbf{r}_i - \mathbf{r}_j) \mathbf{F}_i^J \cdot \mathbf{F}_j^J + \sum_J c_{JJ+2} \sum_{1 \leq i \leq N_J} \sum_{1 \leq j \leq N_{J+}} \delta(\mathbf{r}_i - \mathbf{r}_j) \mathbf{F}_i^J \cdot \mathbf{F}_j^{J+}$. When \mathfrak{S} is given, the coefficients $d_{S_{AB}}$ can be obtained via a diagonalization of H_{spin} in the space expanded by $\Psi_{\mathfrak{S}, S_{AB}}$. The matrix elements are

$$\begin{aligned} \langle \Psi_{\mathfrak{S}, S'_{AB}} | H_{\text{spin}} | \Psi_{\mathfrak{S}, S_{AB}} \rangle &\equiv H_{S'_{AB}, S_{AB}} \\ &= \delta_{S'_{AB} S_{AB}} \left[\sum_J \frac{1}{2} \int \varphi_J^4 \mathbf{dr} c_{J2} (T_J - 2N_J) + \int \varphi_A^2 \varphi_B^2 \mathbf{dr} c_{AB2} \frac{T_{AB} - T_A - T_B}{2} \right] \\ &\quad + \int \varphi_B^2 \varphi_C^2 \mathbf{dr} c_{BC2} \sum_{S_{BC}} \bar{w}(S_A S_B S S_C; S_{AB} S_{BC}) \bar{w}(S_A S_B S S_C; S'_{AB} S_{BC}) \frac{1}{2} (T_{BC} - T_B - T_C) \\ &\quad + \int \varphi_C^2 \varphi_A^2 \mathbf{dr} c_{CA2} \sum_{S_{CA}} (-1)^{S'_{AB} + S_{AB}} \bar{w}(S_B S_A S S_C; S_{AB} S_{CA}) \\ &\quad \bar{w}(S_B S_A S S_C; S'_{AB} S_{CA}) \frac{1}{2} (T_{CA} - T_C - T_A), \end{aligned} \quad (23)$$

where the summation of J covers A, B and C , $\bar{w}(S_A S_B S S_C; S_{AB} S_{BC}) = \sqrt{(2S_{AB} + 1)(2S_{BC} + 1)} w(S_A S_B S S_C; S_{AB} S_{BC})$, the latter is the W-coefficients of Racah, $T_J = S_J(S_J + 1)$, and so on.

Carrying out the diagonalization, the lowest eigenstate is $\Psi_{\mathfrak{S}}$ and the corresponding energy is denoted as $E_{\mathfrak{S}}$. Let the four presumed values in \mathfrak{S} be varied within a reasonable scope. When $\mathfrak{S} = \mathfrak{S}_0$, if $E_{\mathfrak{S}}$ arrives at its minimum, then the g.s. $\Psi_0 = \Psi_{\mathfrak{S}_0}$.

To extract information on spin-texture from Ψ_0 , we calculate the averaged angle between the two spins S_A and S_B as

$$\bar{\theta}_{AB} \equiv \cos^{-1} [\langle \Psi_0 | \hat{S}_A \cdot \hat{S}_B | \Psi_0 \rangle / \sqrt{\langle \Psi_0 | \hat{S}_A^2 | \Psi_0 \rangle \langle \Psi_0 | \hat{S}_B^2 | \Psi_0 \rangle}] = \cos^{-1} \left[\frac{1}{2\sqrt{T_A T_B}} \sum_{S_{AB}} d_{S_{AB}}^2 (T_{AB} - T_A - T_B) \right], \quad (24)$$

where $\hat{S}_J \equiv \sum_i \mathbf{F}_i^J$ is the operators for the total spin of the J -species. Similarly, we have

$$\bar{\theta}_{BC} = \cos^{-1} \left[\frac{1}{2\sqrt{T_B T_C}} \sum_{S_{AB}, S'_{AB}, S_{BC}} d_{S_{AB}} d_{S'_{AB}} \bar{w}(S_A S_B S S_C; S_{AB} S_{BC}) \bar{w}(S_A S_B S S_C; S'_{AB} S_{BC}) (T_{BC} - T_B - T_C) \right], \quad (25)$$

$$\bar{\theta}_{CA} = \cos^{-1} \left[\frac{1}{2\sqrt{T_A T_C}} \sum_{S_{AB}, S'_{AB}, S_{CA}} d_{S_{AB}} d_{S'_{AB}} (-1)^{S'_{AB} + S_{AB}} \bar{w}(S_B S_A S S_C; S_{AB} S_{CA}) \bar{w}(S_B S_A S S_C; S'_{AB} S_{CA}) (T_{CA} - T_C - T_A) \right]. \quad (26)$$

Examples are given below.

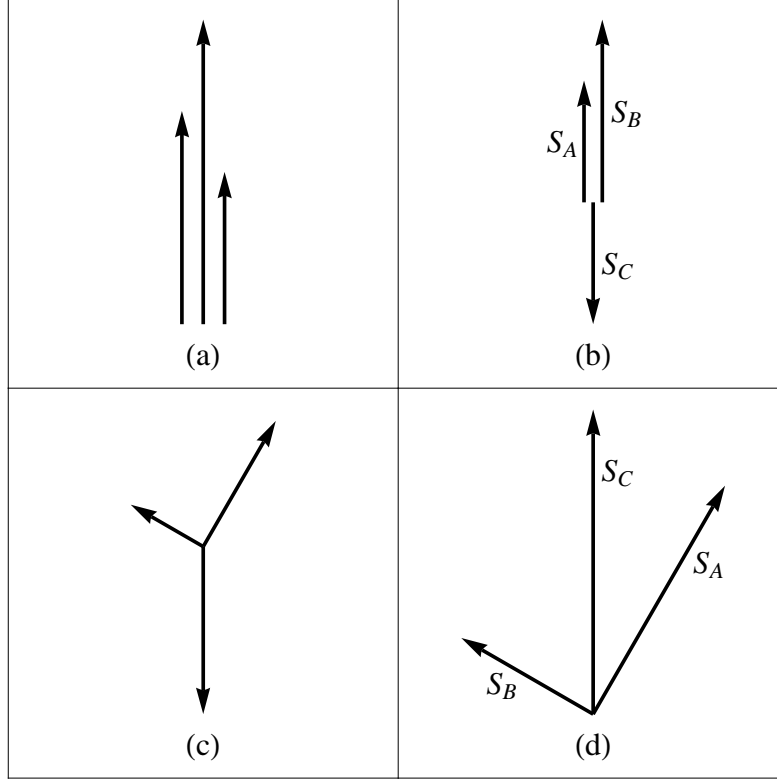


Figure 2. Intuitive pictures of the coplanar spin-textures, where the relative orientations of the spins S_A , S_B and S_C are shown.

Classical model (Type-I)

The total energy of the g.s. can be divided as $E = E_o + E_{\text{spin}}$, where

$$E_{\text{spin}} = \langle \Psi_o | H_{\text{spin}} | \Psi_o \rangle = \sum_J Q_J \langle \Xi | \hat{S}_J^2 - 2N_J | \Xi \rangle + 2 \sum_J Q_{JJ_+} \langle \Xi | \hat{\mathbf{S}}_J \cdot \hat{\mathbf{S}}_{J_+} | \Xi \rangle, \quad (27)$$

where $Q_J = \int \varphi_J^\dagger \mathbf{dr} c_{J2}/2$, $Q_{JJ_+} = \int \varphi_J^2 \varphi_{J_+}^2 \mathbf{dr} c_{JJ_+2}/2$.

To see clearer the physical picture, we propose a classical model to facilitate qualitative analysis. In this model, the total spin of the J -species is considered as a vector \vec{S}_J with norm S_J ranging from 0 to N_J , θ_{JJ_+} is the angle between \vec{S}_J and \vec{S}_{J_+} . The magnitudes and orientations of the three \vec{S}_J together describe an intuitive picture of the spin-texture. The classical analog of E_{spin} is defined as

$$E_{\text{spin}}^M = \sum_J Q_J S_J^2 + 2 \sum_J Q_{JJ_+} S_J S_{J_+} \cos \theta_{JJ_+}, \quad (28)$$

The effect of the inter-species force is embodied by Q_{JJ_+} . When $Q_{JJ_+} < 0$ (attractive), \vec{S}_J and \vec{S}_{J_+} will be lying along the same direction. Whereas when $Q_{JJ_+} > 0$ (repulsive), along opposite directions. Note that, for three spins, two of them will define a plane and will pull the third lying on the same plane. Therefore, the spin-textures of 3-species condensates are assumed to be coplanar (this assumption will be checked later). Thus, in what follows, $\theta_{AB} + \theta_{BC} + \theta_{CA} = 2\pi$ is given. Accordingly, When $\{Q_J\}$ and $\{Q_{JJ_+}\}$ are given, E_{spin}^M is a function of five variables ($S_A, S_B, S_C, \theta_{BC}, \theta_{CA}$). When these variables lead to the minimum of E_{spin}^M , they specify a coplanar spin-texture of the g.s.. In order to find out the minimum, we calculate the partial derivatives of E_{spin}^M . They are given in the appendix.

There are two types of spin-textures. When all $\{Q_{JJ_+}\}$ are negative, \vec{S}_A , \vec{S}_B and \vec{S}_C would tend to be parallel to each others, i.e., all $\cos \theta_{JJ_+} = 1$ as shown in Fig.2a. When only one of $\{Q_{JJ_+}\}$ is negative, say, Q_{AB} is negative, orientations of the spins are shown in Fig.2b, where $\cos \theta_{AB} = 1$, $\cos \theta_{BC} = \cos \theta_{CA} = -1$. These two cases are called in Type-I.

For Type-I, the total energy appears as

$$E_{\text{spin}}^M = \sum_J (Q_J S_J^2 - 2|Q_{JJ_+}| S_J S_{J_+}). \quad (29)$$

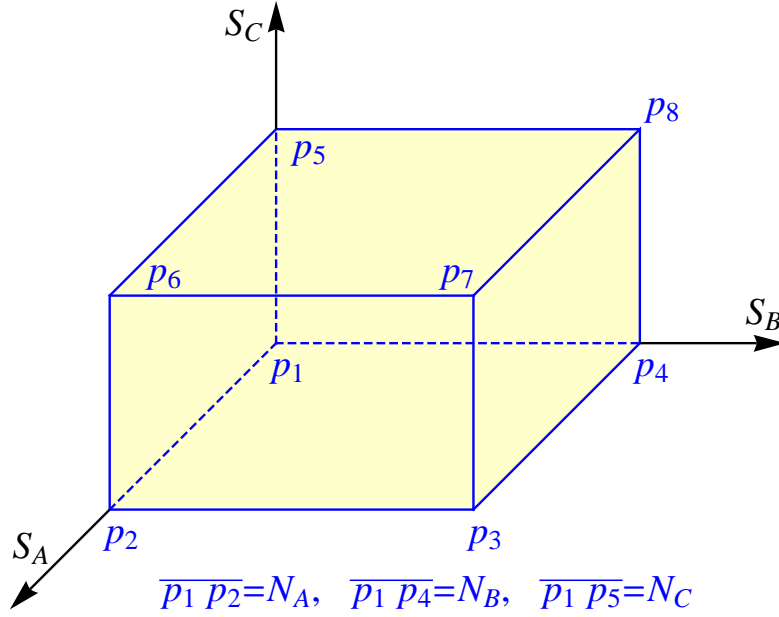


Figure 3. (color online) The cuboid formed by the norms of the three spins S_A , S_B , and S_C each from 0 to N_J .

Let p denotes a point in the 3-dimensional coordinate-space with the coordinates (S_A, S_B, S_C) . This point is bound by a cuboid as shown in Fig.3. When S_J of a species is given, the phase of the species is denoted, for short, by p , f and q if $S_J = 0$, N_J and in between. Let $p_{g.s.}$ be the point where E_{spin}^M arrives at its minimum. There are the following possibilities:

The case $p_{g.s.}$ is located inside the cuboid (i.e., not on the surfaces, edges and vertexes).

In this case $0 < S_J < N_J$ for all J . At the minimum the three equations $\frac{\partial E_{\text{spin}}^M}{\partial S_J} |_{p_{g.s.}} = 0$ are necessary to hold. This leads to a set of homogeneous linear equations for (S_A, S_B, S_C) as

$$Q_J S_J - |Q_{J-J}| S_{J-} - |Q_{J+}| S_{J+} = 0, \quad (J = A, B, C) \quad (30)$$

However, the matrix of this set is in general not singular. Therefore, there is no nonzero solution. Even, for a specific choice of the parameters, the matrix is singular, the nonzero solution can be multiplied by a variable common number ζ . One can see that E_{spin}^M varies with ζ monotonically. In order to minimize E_{spin}^M , ζ should be given either in its upper or lower limit but not inside. Thus, $p_{g.s.}$ cannot locate inside the cuboid. It implies that the three species cannot all in the q -phase.

Let a rectangle on the surface of the cuboid be denoted as $p_1 p_4 p_8 p_5$, etc. (refer to Fig.3). There are six rectangles, three of them contain p_1 as a vertex (the first kind), the other three contain p_7 as a vertex (the second kind).

The case $p_{g.s.}$ is located on a rectangle of the first kind.

There are three such rectangles. If $p_{g.s.}$ were located on $p_1 p_4 p_8 p_5$ (i.e., $S_A = 0$, $0 \leq S_B \leq N_B$, and $0 \leq S_C \leq N_C$), it is necessary to have $\frac{\partial E_{\text{spin}}^M}{\partial S_A} |_{p_{g.s.}} \geq 0$. However, this leads to $-|Q_{AB}| S_B - |Q_{CA}| S_C \geq 0$ which cannot be realized unless $S_B = S_C = 0$. With similar arguments, $p_{g.s.}$ cannot located on $p_1 p_5 p_6 p_2$ and $p_1 p_2 p_3 p_4$ as well, but it can locate at the point p_1 . Thus this case is prohibited unless $p_{g.s.} = p_1$. It implies that the case with one or two species in p -phase is prohibited, while all species in p is possible. This fact coincides with the finding found in 2-species condensates, in which the p -phase is extremely fragile when it is accompanied by an f or a q . Therefore, the $p+f$ or $p+q$ textures do not exist, but the $p+p$ texture is allowed¹⁴⁻¹⁷).

With the above prohibitions, $p_{g.s.}$ can only access p_1 , p_7 , the interior of the three rectangles of the second kind, and the interior of the three edges $\overline{p_7 p_6}$, $\overline{p_7 p_3}$, and $\overline{p_7 p_8}$.

The case $p_{g.s.} = p_7$.

In this case $S_J = N_J$ for all J and, accordingly, the texture is denoted as $f//f//f$. (the symbol $//$ implies that the related spins are either parallel or anti-parallel). The three inequalities $\frac{\partial E_{\text{spin}}^M}{\partial S_J} |_{p_7} < 0$ are required to hold. This leads to the constraints imposed on the parameters as listed at the right of the first row of Tab.1. These constraints give the scope of the parameters that supports

the $f//f//f$ -texture. The energy of this texture $E_{\text{spin}}^{\text{M}} = E_{fff}^{\text{M}}$ is listed in Tab.2. In these tables, we have defined

$$\alpha_{JJ_+} \equiv Q_J Q_{J_+} - |Q_{JJ_+}|^2, \quad (31)$$

and

$$\alpha_{ABC} \equiv Q_A Q_B Q_C - 2|Q_{AB}||Q_{BC}||Q_{CA}| - Q_A Q_{BC}^2 - Q_B Q_{CA}^2 - Q_C Q_{AB}^2. \quad (32)$$

When every species is ferromagnetic in nature (i.e., all $Q_J < 0$), the inequality $N_J Q_J - N_{J_-} |Q_{J_- J}| - N_{J_+} |Q_{JJ_+}| < 0$ holds definitely, and the $f//f//f$ texture is the only choice for the g.s.. When some species (say, J -species) is polar in nature (i.e., $Q_J > 0$), the term $N_J Q_J$ (representing the intra-interaction) and the other two terms (representing the combined inter-interaction) are competing. Only when $|Q_{J_- J}|$ and $|Q_{JJ_+}|$ are sufficiently large the J -species could be in f -phase. Note that, in Q_J , the strength c_{J2} is weighted by $\int \phi_J^4 d\mathbf{r}/2$, while in $Q_{JJ'}$, $c_{JJ'2}$ is weighted by $\int \phi_J^2 \phi_{J'}^2 d\mathbf{r}/2$. Thus, the profiles of the spatial wave functions are important to the spin-textures.

Table 1. When all $Q_{JJ_+} < 0$ or only one $Q_{JJ_+} < 0$, the representative possible spin-textures of the g.s. are listed in the first column. The notation $f//f//q$ implies that the A , B and C species are in f , f and q , respectively. The three spins S_A , S_B and S_C are either parallel or anti-parallel to each others. The (in)equalities listed in the second column impose a constraint on the parameters so that the associated texture can emerge only in a subspace in the parameter space. In the first row $J = A, B$ and C . (J_-, J, J_+) is a cyclic permutation of (A, B, C) . The constraints for other possible textures not listed in the table, say, $f//q//f$, can be obtained by a cyclic permutation of the indexes A , B and C .

| spin-texture | constraint |
|--------------|--|
| $f//f//f$ | $N_J Q_J - N_{J_-} Q_{J_- J} - N_{J_+} Q_{JJ_+} < 0$ |
| $f//f//q$ | $N_A Q_A - N_B Q_{AB} - S_C Q_{CA} < 0$ $N_B Q_B - S_C Q_{BC} - N_A Q_{AB} < 0$ $S_C Q_C - (N_A Q_{CA} + N_B Q_{BC}) = 0$ $Q_C > 0$ |
| $f//q//q$ | $N_A Q_A - S_B Q_{AB} - S_C Q_{CA} < 0$ $S_B = N_A (Q_C Q_{AB} + Q_{BC} Q_{CA}) / \alpha_{BC}$ $S_C = N_A (Q_B Q_{CA} + Q_{BC} Q_{AB}) / \alpha_{BC}$ $Q_B > 0, Q_C > 0, \alpha_{BC} > 0$ |
| $p+p+p$ | $\alpha_{ABC} \geq 0, Q_A > 0, Q_B > 0, Q_C > 0$ |

Table 2. The model energies of the g.s. in various textures.

| model | energy |
|----------------------|--|
| E_{fff}^{M} | $\sum_J (Q_J N_J^2 - 2 Q_{JJ_+} N_J N_{J_+})$ |
| E_{ffq}^{M} | $\frac{1}{Q_C} [N_A^2 \alpha_{CA} + N_B^2 \alpha_{BC} - 2N_A N_B (Q_C Q_{AB} + Q_{BC} Q_{CA})]$ |
| E_{fqq}^{M} | $\frac{N_A^2}{\alpha_{BC}} \alpha_{ABC}$ |
| E_{ppp}^{M} | 0 |

The case $p_{\text{g.s.}}$ is located in the interior of $\overline{p_7 p_6}$, $\overline{p_7 p_3}$ or $\overline{p_7 p_8}$.

When $p_{\text{g.s.}}$ is in the interior of $\overline{p_7 p_3}$, $S_A = N_A$, $S_B = N_B$, and $0 < S_C < N_C$. The associated texture is $f//f//q$. The two inequalities $\frac{\partial E_{\text{spin}}^{\text{M}}}{\partial S_A} |_{p_{\text{g.s.}}} < 0$ and $\frac{\partial E_{\text{spin}}^{\text{M}}}{\partial S_B} |_{p_{\text{g.s.}}} < 0$, together with $\frac{\partial E_{\text{spin}}^{\text{M}}}{\partial S_C} |_{p_{\text{g.s.}}} = 0$ and $\frac{\partial^2 E_{\text{spin}}^{\text{M}}}{\partial S_C^2} |_{p_{\text{g.s.}}} > 0$ are required. This leads to the constraint listed in the second row of Tab.1. This texture can be realized only if $Q_C > 0$ (i.e., the C -species is polar in nature), whereas Q_A and Q_B can be negative or weakly positive. If they are positive and large, the inter-species interaction should be

even stronger to ensure that the inequalities hold. The equality for S_C implies that the intra-force and the inter-force imposed on the C -atoms arrive at a balance. The energy E_{ffq}^M is given in Tab.2. The textures $fllqllf$ and $qllfllf$ can be similarly discussed. These three together are called the double- f -texture (double- f -tex).

The case $p_{g.s.}$ is located in the interior of the rectangles of the second kind.

When $p_{g.s.}$ is in the interior of $p_7p_6p_2p_3$, $S_A = N_A$, $0 < S_B < N_C$, and $0 < S_C < N_C$. The associated texture is $fllqllq$. The inequality $\frac{\partial E_{spin}^M}{\partial S_A}|_{p_{g.s.}} < 0$ together with $\frac{\partial E_{spin}^M}{\partial S_J}|_{p_{g.s.}} = 0$ and $\frac{\partial^2 E_{spin}^M}{\partial S_J^2}|_{p_{g.s.}} > 0$ ($J = B$ and C) are required. This leads to the constraint listed in the third row of Tab.1. This texture can be realized only if both the B - and C -species are polar in nature, whereas Q_A can be negative or weakly positive. Besides, the condition $Q_B Q_C > |Q_{BC}|^2$ is necessary. One can prove that the constraint listed in the third row leads to $\alpha_{ABC} < 0$. Note that $E_{ppp}^M = 0$ while E_{ffq}^M is a product of a positive value and α_{ABC} . Thus, $\alpha_{ABC} < 0$ is a necessary condition for the $fllqllq$ texture. The textures $qllfllq$ and $qllqllf$ can be similarly discussed. The three together are called the single- f -tex.

The case $p_{g.s.}$ is located at p_1 .

When all the three species are polar in nature ($Q_A > 0$, $Q_B > 0$, $Q_C > 0$) and the inter-species forces are zero or weak, the first term of α_{ABC} , $Q_A Q_B Q_C$, is positive and is dominant. This leads to $\alpha_{ABC} \geq 0$. In this case all the species are in p and the texture is therefore denoted as $p+p+p$. When $\{|Q_{JJ_+}|\}$ increases, α_{ABC} will decrease. Once α_{ABC} becomes zero, the energy of the single- f -tex will be lower than E_{ppp}^M (refer to Tab.2), and the transition from $p+p+p$ to the single- f -tex will occur.

With these in mind, the $g.s.$ is either in the $p+p+p$ or in a texture without p but with at least one species in f .

Spin-texture transition

We aim at the effect caused by the variation of the inter-species forces. Note that the effect of Q_{JJ_+} is to pull the spins of the J and J_+ species lying along the same direction (opposite directions) if $Q_{JJ_+} < 0$ (> 0). Therefore, in general, a stronger $|Q_{JJ_+}|$ will cause the appearance of the f -phase. Starting from $\{|Q_{JJ_+}|\} = 0$, the first transition is from $p+p+p$ to a single- f -tex as mentioned above. Recall that the single- f -tex must have $\alpha_{ABC} \leq 0$ while the $p+p+p$ has $\alpha_{ABC} > 0$, therefore $\alpha_{ABC} = 0$ is the critical point of transition. Since α_{ABC} is invariant under cyclic permutation of the indexes, this critical point is common to all $p+p+p \rightarrow$ single- f -tex transitions disregarding which species is in f . One can prove that the three sets of constraint for the three single- f -texas do not compromise with each others, i.e., for a given set of parameters, the two sets of constraint for two different single- f -texas cannot both be satisfied. If both were satisfied, the combined constraints would lead to $\alpha_{ABC} > 0$, and therefore in contradiction with the common feature $\alpha_{ABC} \leq 0$. This fact implies that, once a single- f -tex appears, the other two cannot appear. Thus, the transitions among the three single- f -texas (say, $fllqllq \rightarrow qllfllq$) are prohibited. Therefore, $p+p+p$ can transit only to a specific single- f -tex, it depends on the parameters.

When $\{|Q_{JJ_+}|\}$ increase further, a q -phase can be changed to an f -phase. Therefore, the single- f -tex \rightarrow double- f -tex transition will occur (as shown below). One can prove that the three sets of (in)equalities for the three double- f -texas do not compromise with each others as before. Thus, a single- f -tex can uniquely transit to a specific double- f -tex, and the transitions among the three double- f -texas are prohibited. When $\{|Q_{JJ_+}|\}$ increases further, eventually, the $g.s.$ must be in the $fllfllf$ texture.

With these in mind the increase of $\{|Q_{JJ_+}|\}$ will lead to a chain of transitions as $p+p+p \rightarrow$ single- f -tex \rightarrow double- f -tex \rightarrow $fllfllf$.

Two numerical examples of Type I are shown in Fig.4 and Fig.5, where the variation of the spin-texture (specified by S_A , S_B , S_C , and θ_{AB} , θ_{BC} , θ_{CA}) against Q_{CA} is plotted. The results from the QM calculation are in solid lines, those from the model are in dotted lines. The coincidence is quite well. In particular, the whole chain of transitions is recovered by the QM calculation and the critical points are one-to-one close to each other. The intuitive pictures shown in Fig.2a and Fig.2b are also supported by Fig.4b and Fig.5b. In Fig.4b the angles are very small ($< 9^\circ$), in Fig.5b the angles are either close to zero or to π . Thus, the analysis based on the model is reliable. Note that the model is symmetric with respect to $Q_{JJ_+} \leftrightarrow -Q_{JJ_+}$. This symmetry can be shown by comparing Fig.4a and Fig.5a.

According to the model, when $|Q_{CA}|$ increases, the transition $p+p+p \rightarrow fllqllq$ occurs at $|Q_{CA}| = q_1$, where $E_{ppp}^M = E_{ffq}^M$. Thus, q_1 is the solution of the equation

$$\alpha_{ABC} = 0. \quad (33)$$

In Fig.4 $q_1 = 0.165$ as listed in Tab.3. Recall that, for a 2-species BEC, the $p+p \rightarrow fllq$ transition will occur when $\alpha_{JJ_+} = 0$ ¹⁵⁻¹⁷. Obviously, Eq.(33) is a generalization of Eq.(31). In both equations the competition of the intra- and inter-interactions is clearly shown.

The transition $fllqllq \rightarrow fllfllq$ occurs at q_2 , where $E_{ffq}^M = E_{ffq}^M$. Thus

$$q_2 = \frac{1}{N_A |Q_{BC}|} (N_B Q_B Q_C - N_B |Q_{BC}|^2 - N_A Q_C |Q_{AB}|). \quad (34)$$

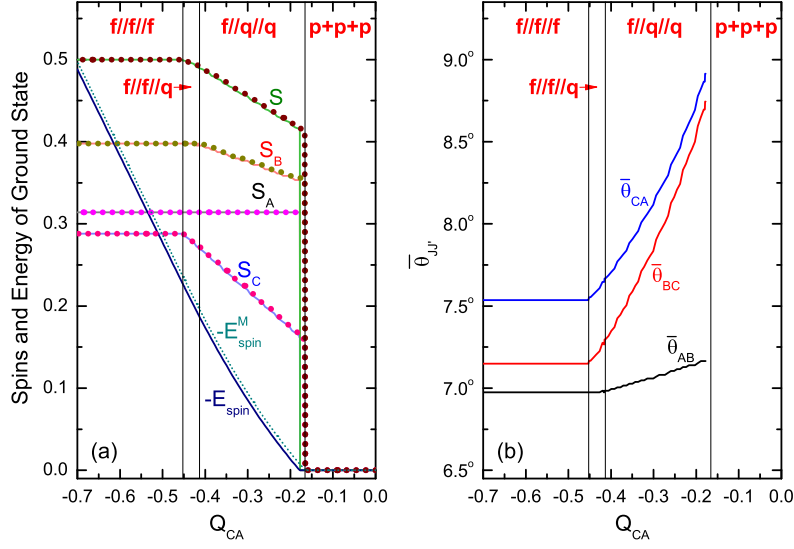


Figure 4. (color online) An example for the variation of the spin-texture of Type-I against Q_{CA} . The texture is specified by S_A/N , S_B/N , S_C/N , and $S/(2N)$ (where $N = N_A + N_B + N_C$) in (a) and by the angles $\bar{\theta}_{AB}$, $\bar{\theta}_{BC}$ and $\bar{\theta}_{CA}$ (in degree) between them (b). The results from the exact diagonalization of H_{spin} are plotted in solid lines. In (a), the results from the model are plotted in dotted lines, and $\theta_{AB} = \theta_{BC} = \theta_{CA} = 0$ are assumed. Accordingly, the classical model has $S = S_{class} \equiv S_A + S_B + S_C$ as shown in (a). The dimensionless parameters are given as $N_A = 120$, $N_B = 152$, $N_C = 110$, $Q_A = 0.6$, $Q_B = 0.5$, $Q_C = 0.77$, $Q_{AB} = -0.46$, $Q_{BC} = -0.2$, Q_{CA} is from -0.7 to 0 . Since all $\{Q_{JJ_+}\}$ are given negative, this example represents the case of Fig.2a.

In Fig.4 $q_2 = 0.414$ as listed in Tab.3.

The transition $f//f//q \rightarrow f//f//f$ occurs at q_3 , where $E_{ffq}^M = E_{fff}^M$. Thus,

$$q_3 = \frac{1}{N_A}(N_C Q_C - N_B |Q_{BC}|). \quad (35)$$

In Fig.4 $q_3 = 0.453$. Recall that, for 2-species BEC with A and C atoms, the $f//q \rightarrow f//f$ transition will occur when $q_3 = \frac{1}{N_A} N_C Q_C$ ¹⁵⁻¹⁷. Thus, the existence of the third species (B-atoms) is helpful to the transition (i.e., the $f//f//f$ texture can be realized at a smaller $|Q_{CA}|$).

It turns out that the critical values predicted by the model are close to the values from QM calculation as shown in Tab.3 (except q_1 , but still acceptable). Thus, the related analytical formulae are useful for qualitative evaluation. For other chains of transition, the analytical formulae of the critical points can be similarly obtained.

Table 3. The critical values of Q_{CA} in the chain $p+p+p \rightarrow f//q//q \rightarrow f//f//q \rightarrow f//f//f$. The other parameters are listed in the caption of Fig.5.

| critical point | classical model | QM calculation |
|----------------|-----------------|----------------|
| q_1 | 0.165 | 0.177 |
| q_2 | 0.414 | 0.419 |
| q_3 | 0.453 | 0.450 |

Classical model (Type-II)

When all Q_{JJ_+} are positive (Fig.2c) or only one of them is positive (Fig.2d, where $Q_{AB} > 0$), the associated spin-textures are in Type-II. In this type the three spins point at different directions, but they are assumed to be coplanar ($\theta_{AB} + \theta_{BC} + \theta_{CA} = 2\pi$). The total energy appears as

$$E_{spin}^M = \sum_J Q_J S_J^2 + 2 \sum_J Q'_{JJ_+} S_J S_{J_+}, \quad (36)$$

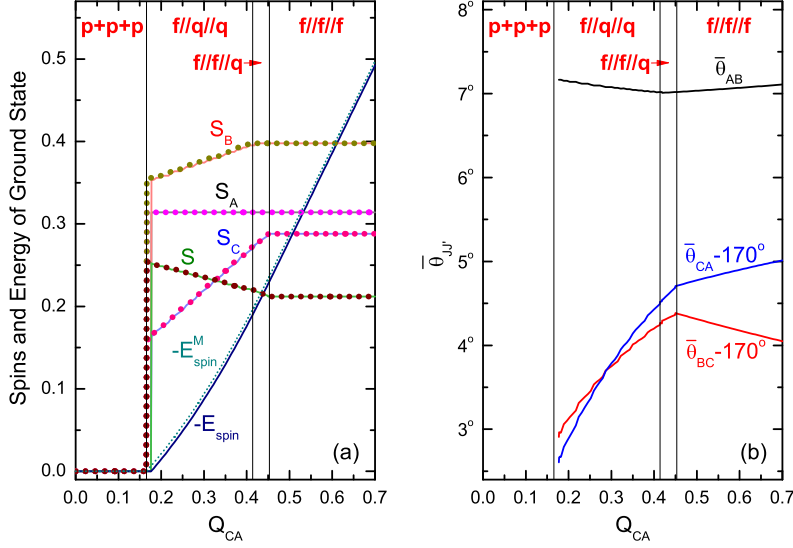


Figure 5. (color online) An example similar to Fig.4 but with $Q_{BC} = 0.2$ and Q_{CA} is from 0 to 0.7. Since only one of $\{Q_{JJ_+}\}$ is given negative ($Q_{AB} = -0.46$), this example represents the case of Fig.2b. Accordingly, in the model, $\theta_{AB} = 0$ and $\theta_{BC} = \theta_{CA} = 180^\circ$ are assumed and $S_{class} \equiv |S_A + S_B - S_C|$ in (a).

where $Q'_{JJ_+} = Q_{JJ_+} \cos \theta_{JJ_+}$.

To find out the point $p_{g.s.}$ where the minimum of E_{spin}^M is located, we first consider the partial derivatives of E_{spin}^M against $\{S_J\}$ when $\{Q_J\}$ and $\{Q'_{JJ_+}\}$ are considered as constants. Thus, the situation is the same as for Type-I. With the same arguments as those for Type-I, we deduce that $p_{g.s.}$ can only access p_1 , the interiors of $\overline{p_7 p_6}$, $\overline{p_7 p_3}$, $\overline{p_7 p_8}$, the interiors of the three rectangles of the second kind, and p_7 .

$p_{g.s.} = p_7$.

In this case every species is fully polarized, but the spins of any two species are in general neither parallel nor antiparallel to each other. Therefore, instead of $f//f//f$, this type of texture is denoted as $f+f+f$. The three inequalities $\frac{\partial E_{spin}^M}{\partial S_J} |_{p_{g.s.}} < 0$ are required which lead to the constraints $N_J Q_J + N_{J-} Q'_{J-} + N_{J+} Q'_{J+} < 0$, where J is for A, B and C . In addition, the two derivatives $\frac{\partial E_{spin}^M}{\partial \theta_{BC}} |_{p_{g.s.}}$ and $\frac{\partial E_{spin}^M}{\partial \theta_{CA}} |_{p_{g.s.}}$ are required to be zero. These lead to (refer to Eqs.(48) and (49))

$$\cos \theta_{BC} = G_{BC}(N_A N_B N_C), \quad (37)$$

$$\cos \theta_{CA} = G_{CA}(N_A N_B N_C). \quad (38)$$

The two angles obtained in this way should ensure that the two second order derivatives given in Eqs.(46) and (47) are positive. When all the $Q_{JJ_+} > 0$, from Eqs.(46) and (47) we know that this requirement could be satisfied if θ_{BC} and θ_{CA} are large enough, thereby the repulsion caused by Q_{JJ_+} is reduced. Whereas when only one, say, $Q_{AB} > 0$ while $Q_{BC} < 0$ and $Q_{CA} < 0$, θ_{BC} and θ_{CA} should be small enough, thereby the attraction caused by Q_{BC} and Q_{CA} can be strengthened. Once the angles are known, the three $Q'_{JJ'}$ are known. Then, the energy $E_{spin}^M = \sum_J Q_J N_J^2 + 2 \sum_J Q'_{JJ_+} N_J N_{J_+} \equiv E_{f+f+f}$ and the subspace of parameters that supports this texture are also known.

$p_{g.s.}$ **locates in the interiors of $\overline{p_7 p_6}$, $\overline{p_7 p_3}$ and $\overline{p_7 p_8}$.**

When $p_{g.s.}$ locates in the interior of $\overline{p_7 p_3}$ as an example, $S_A = N_A$, $S_B = N_B$, and the texture is denoted as $f+f+q$. The constraints appear as (refer to the second row of Tab.1):

$$\begin{cases} N_A Q_A + N_B Q'_{AB} + S_C Q'_{CA} < 0 \\ N_B Q_B + S_C Q'_{BC} + N_A Q'_{AB} < 0 \\ S_C Q_C + (N_A Q'_{CA} + N_B Q'_{BC}) = 0 \end{cases}, \quad (39)$$

The angles are subjected to the two coupled equations (refer to Eqs.(48) and (49))

$$\cos \theta_{BC} = G_{BC}(N_A, N_B, -(N_A Q'_{CA} + N_B Q'_{BC})/Q_C), \quad (40)$$

$$\cos \theta_{CA} = G_{CA}(N_A, N_B, -(N_A Q'_{CA} + N_B Q'_{BC})/Q_C), \quad (41)$$

where the angles are also contained in Q'_{JJ_+} . Solving these equations (say, numerically), we can obtain θ_{BC} and θ_{CA} . Then, the energy E_{f+f+q} and the subspace of parameters that supports this texture can be known as before. The cases of $f+q+f$ and $q+f+f$ can be similarly discussed.

p.g.s. locates in the interiors of the rectangles of the second kind.

For the rectangle $p_7p_6p_2p_3$ as an example, $S_A = N_A$, the texture is denoted as $f+q+q$. The constraint imposed on this texture is listed in the third row of Tab.1 but with $-|Q_{JJ_+}|$ being replaced by Q'_{JJ_+} . In addition, the two coupled equations

$$\cos \theta_{BC} = G_{BC}(N_A S_B S_C), \quad (42)$$

$$\cos \theta_{CA} = G_{CA}(N_A S_B S_C), \quad (43)$$

are required to be satisfied. Then S_B, S_C , together with the angles can be known, thereby E_{f+q+q}^M is known.

$p_{g.s.} = p_1$.

When all $Q_J > 0$ and when the strengths of the inter-species interaction become weaker, all the three E_{f+q+q}^M, E_{q+f+q}^M , and E_{q+q+f}^M will be larger than zero, in this case $p_{g.s.} = p_1$ and the texture is $p+p+p$.

A comparison of the results from the model and from the diagonalization of H_{spin} is shown in Tab.4.

Table 4. For the texture $f+f+f$ of the Type-II., the angles (in degrees) between the spins against the increase of Q_{CA} . The data for θ_{JJ_+} are from the model (refer to Eqs.(37) and (38)), those for $\bar{\theta}_{JJ_+}$ are from the diagonalization of H_{spin} (refer to Eqs.(24), (25) and (26)). The parameters are given as $N_A = 120, N_B = 152, N_C = 110, Q_A = -0.6, Q_B = -0.5, Q_C = -0.77, Q_{AB} = 0.3, Q_{BC} = 0.4, Q_{CA}$ is from 0.3 to 0.8.

| Q_{CA} | θ_{CA} | $\bar{\theta}_{CA}$ | θ_{BC} | $\bar{\theta}_{BC}$ | θ_{AB} | $\bar{\theta}_{AB}$ | $\bar{\theta}_{CA} + \bar{\theta}_{BC} + \bar{\theta}_{AB}$ |
|----------|---------------|---------------------|---------------|---------------------|---------------|---------------------|---|
| 0.3 | 81.6 | 81.8 | 144.2 | 144.0 | 134.3 | 134.1 | 359.9 |
| 0.4 | 111.3 | 111.1 | 132.7 | 132.5 | 116.0 | 116.4 | 360.0 |
| 0.5 | 126.9 | 126.7 | 127.9 | 127.6 | 105.3 | 105.5 | 359.8 |
| 0.6 | 136.8 | 136.7 | 125.8 | 125.5 | 97.5 | 97.6 | 359.8 |
| 0.7 | 143.7 | 143.5 | 125.1 | 124.7 | 91.2 | 91.6 | 359.8 |
| 0.8 | 148.9 | 148.5 | 125.3 | 124.6 | 85.8 | 86.6 | 359.7 |

Tab.4 demonstrates that the results given by Eqs.(24), (25) and (26) are quite accurate. In particular, the sum of the three $\{\bar{\theta}_{JJ_+}\}$ given in the last column is very close to 2π . This supports the assumption of coplanar texture.

Final remarks

Features of the spin-textures of 3-species condensates with spin-1 atoms have been extracted from a model and have been checked via QM calculation. The results from the model are found to be valid. In summary:

- The textures can be described by the norms of the three spins $\{S_J\}$ and the average angles $\{\bar{\theta}_{JJ_+}\}$ between them. When the three species are polar in nature (i.e., all $c_{J2} > 0$) and the inter-forces are weak, $\{S_J\}$ can all be zero ($p+p+p$). Otherwise, they are all nonzero and essentially lying on a plane.
- The spin-textures not in $p+p+p$ can be first classified according to the relative orientations of $\{S_J\}$ as intuitively shown in Fig.2. When all inter-forces are attractive (i.e., all $c_{JJ'2} < 0$), the texture is shown in Fig.2a where all spins point to the same direction. When only one is attractive (say, $c_{AB2} < 0$), shown in Fig.2b. When all are repulsive (all $c_{JJ'2} > 0$), shown in Fig.2c. When only one is repulsive (say, $c_{AB2} > 0$), shown in Fig.2d.
- The spin-textures can be further classified according to the norms of the spin. In addition to $p+p+p$, there are other three textures, namely, the single- f -tex (where one species is in f , i.e., fully polarized), the double- f -tex (two species in f), and the $f+f+f$ (all in f). Note that the single- p -tex, the double- p -tex, and the $q+q+q$ do not exist. Thus, the coexistence of a p and an f (or a q) is not allowed. If not in $p+p+p$, at least a species must be fully polarized.

- Starting from the $p+p+p$, when $|c_{JJ'}|$ increases, more species will tend to be in f -phase. Therefore, a chain of phase-transitions $p+p+p \rightarrow f+q+q \rightarrow f+f+q \rightarrow f+f+f$ will occur. In the parameter space, there are a number of critical surfaces. When the point (representing a set of parameters) vary and pass through one of the surfaces, a transition will occur. For Type-I (Fig.2a and Fig.2b) the equations describing the surfaces have been quite accurately obtained (refer to Eqs.(33), (34) and (35)). Thus, the critical points at which the transitions occur can be predicted. Moreover, the analytical formulae demonstrate the competition among contradicting physical factors, thereby the inherent physics could be understood better. For Type-II (Fig.2c and Fig.2d), analytical analysis based on the model becomes complicated. Nonetheless, the results from the model have been checked to be also valid.

Acknowledgements

Supported by the National Natural Science Foundation of China under Grants No.11372122, 11274393, 11574404, and 11275279; the Open Project Program of State Key Laboratory of Theoretical Physics, Institute of Theoretical Physics, Chinese Academy of Sciences, China(No.Y4KF201CJ1); the National Basic Research Program of China (2013CB933601); and the Natural Science Foundation of Guangdong of China (2016A030313313).

Appendix

From the total energy of the model given in Eq.(28) we have the derivatives:

$$\frac{\partial E_{\text{spin}}^{\text{M}}}{\partial \theta_{BC}} = -2[S_A S_B Q_{AB} \sin(\theta_{BC} + \theta_{CA}) + S_B S_C Q_{BC} \sin \theta_{BC}], \quad (44)$$

$$\frac{\partial E_{\text{spin}}^{\text{M}}}{\partial \theta_{CA}} = -2[S_A S_B Q_{AB} \sin(\theta_{BC} + \theta_{CA}) + S_C S_A Q_{CA} \sin \theta_{CA}], \quad (45)$$

$$\frac{\partial^2 E_{\text{spin}}^{\text{M}}}{\partial \theta_{BC}^2} = -2[S_A S_B Q_{AB} \cos(\theta_{BC} + \theta_{CA}) + S_B S_C Q_{BC} \cos \theta_{BC}], \quad (46)$$

$$\frac{\partial^2 E_{\text{spin}}^{\text{M}}}{\partial \theta_{CA}^2} = -2[S_A S_B Q_{AB} \cos(\theta_{BC} + \theta_{CA}) + S_C S_A Q_{CA} \cos \theta_{CA}]. \quad (47)$$

Note that the coupled equations $\frac{\partial E_{\text{spin}}^{\text{M}}}{\partial \theta_{BC}} = 0$ and $\frac{\partial E_{\text{spin}}^{\text{M}}}{\partial \theta_{CA}} = 0$ have a trivial solution: both θ_{BC} and θ_{CA} are equal to 0 or π , and a non-trivial solution as

$$\cos \theta_{BC} = G_{BC}(S_A S_B S_C) \equiv \frac{(S_A Q_{AB} Q_{CA})^2 - (S_B Q_{AB} Q_{BC})^2 - (S_C Q_{BC} Q_{CA})^2}{2S_B S_C Q_{AB} Q_{BC}^2 Q_{CA}}, \quad (48)$$

$$\cos \theta_{CA} = G_{CA}(S_A S_B S_C) \equiv \frac{-(S_A Q_{AB} Q_{CA})^2 + (S_B Q_{AB} Q_{BC})^2 - (S_C Q_{BC} Q_{CA})^2}{2S_A S_C Q_{AB} Q_{BC} Q_{CA}^2}. \quad (49)$$

Besides, one can prove the following useful relation

$$\sin \theta_{CA} = \frac{S_B Q_{BC}}{S_A Q_{CA}} \sin \theta_{BC}. \quad (50)$$

We further have

$$\frac{\partial E_{\text{spin}}^{\text{M}}}{\partial S_J} = 2[Q_J S_J + Q_{J-J} \cos \theta_{J-J} S_{J-} + Q_{J+} \cos \theta_{J+} S_{J+}], \quad (J = A, B, C) \quad (51)$$

$$\frac{\partial^2 E_{\text{spin}}^{\text{M}}}{\partial S_J^2} = 2Q_J. \quad (52)$$

The above partial derivatives of $E_{\text{spin}}^{\text{M}}$ are essential in the search of the g.s..

References

1. Stamper-Kurn, D. M., Andrews, M. R., Chikkatur, A. P., Inouye, S., Miesner, H. J., Stenger, J. and Ketterle, W., Optical Confinement of a Bose-Einstein Condensate, *Phys. Rev. Lett.* **80**, 2027 (1998).

2. Ho, T. L., Spinor Bose Condensates in Optical Traps, *Phys. Rev. Lett.* **81**, 742 (1998).
3. Law, C. K., Pu, H. and Bigelow, N. P., Quantum Spins Mixing in Spinor Bose-Einstein Condensates, *Phys. Rev. Lett.* **81**, 5257 (1998).
4. Goldstein, Elena V. and Meystre, Pierre, Quantum theory of atomic four-wave mixing in Bose-Einstein condensates, *Phys. Rev. A* **59**, 3896 (1999).
5. Ho, T. L. and Yip, S. K., Fragmented and Single Condensate Ground States of Spin-1 Bose Gas, *Phys. Rev. Lett.* **84**, 4031 (2000).
6. Koashi, M. and Ueda, M., Exact Eigenstates and Magnetic Response of Spin-1 and Spin-2 Bose-Einstein Condensates, *Phys. Rev. Lett.* **84**, 1066 (2000).
7. Luo, M., Li, Z. B. and Bao, C. G., Bose-Einstein condensate of a mixture of two species of spin-1 atoms, *Phys. Rev. A* **75**, 043609 (2007).
8. Xu, Z. F., Lü, R. and You, L., Quantum entangled ground states of two spinor Bose-Einstein condensates, *Phys. Rev. A* **84**, 063634 (2011).
9. Shi, Yu and Ge, Li, Three-dimensional quantum phase diagram of the exact ground states of a mixture of two species of spin-1 Bose gases with interspecies spin exchange, *Phys. Rev. A* **83**, 013616 (2011).
10. Shi, Yu and Ge, Li, Ground states of a mixture of two species of spin-1 Bose gases with interspecies spin exchange in a magnetic field, *Int. J. Mod. Phys. B* **26**, 1250002 (2012).
11. Xu, Z. F., Mei, J. W., Lü, R. and You, L., Spontaneously axisymmetry-breaking phase in a binary mixture of spinor Bose-Einstein condensates, *Phys. Rev. A* **82**, 053626 (2010).
12. Zhang, J., Li, T. T. and Zhang, Yunbo, Interspecies singlet pairing in a mixture of two spin-1 Bose condensates, *Phys. Rev. A* **83**, 023614 (2011).
13. Irikura, Naoki, Eto, Yujiro, Hirano, Takuya and Saito, Hiroki, Ground-state phases of a mixture of spin-1 and spin-2 Bose-Einstein condensates, *Phys. Rev. A* **97**, 023622 (2018).
14. Shi, Yu, Ground states of a mixture of two species of spinor Bose gases with interspecies spin exchange, *Phys. Rev. A* **82**, 023603 (2010).
15. He, Y. Z., Liu, Y. M. and Bao, C. G., Variation of the spin textures of 2-species spin-1 condensates studied beyond the single spatial mode approximation and the experimental identification of these textures, *Phys. Scr.* **94**, 115403 (2019).
16. Xu, Z. F., Zhang, Yunbo and You, L., Binary mixture of spinor atomic Bose-Einstein condensates, *Phys. Rev. A* **79**, 023613 (2009).
17. He, Y. Z., Liu, Y. M. and Bao, C. G., Spin-Textures of the Condensates with Two Kinds of Spin-1 Atoms Studied Beyond the Single Spatial Mode Approximation, *J. Low Temp. Phys.* **196**, 458-472 (2019).
18. Katriel, J., Weights of the total spins for systems of permutational symmetry adapted spin-1 particles, *Journal of Molecular Structure: THEOCHEM* **547**, 1-11 (2001).
19. J.Polo, *et al.*, Analysis beyond the Thomas-Fermi approximation of the density profiles of a miscible two-component Bose-Einstein condensate, *Phys. Rev. A* **91**, 053626 (2015).
20. He, Y. Z., Liu, Y. M. and Bao, C. G., Generalized Gross-Pitaevskii equation adapted to the $U(5) \supset SO(5) \supset SO(3)$ symmetry for spin-2 condensates, *Phys. Rev. A* **91**, 033620 (2015).
21. Liu, Y. M., He, Y. Z. and Bao, C. G., Singularity in the matrix of the coupled Gross-Pitaevskii equations and the related state-transitions in three-species condensates, *Scientific reports* **7**, 6585 (2017).
22. Li, Z. B., Liu, Y. M., Yao, D. X. and Bao, C. G., Two types of phase diagrams for two-species Bose-Einstein condensates and the combined effect of the parameters, *J. Phys. B: At. Mol. Opt. Phys.* **50**, 135301 (2017).
23. Bao, C. G. and Li, Z. B., Ground band and a generalized Gross-Pitaevskii equation for spinor Bose-Einstein condensates, *Phys. Rev. A* **70**, 043620 (2004).

Author contributions

Y. Z. He is responsible to the numerical calculation. Y. M. Liu is responsible to the theoretical derivation. C. G. Bao provides the idea, write the paper, and responsible to the whole paper. All authors reviewed the manuscript.

Additional information

Competing Interests: The authors declare that they have no competing interests.